

SEISMIC ISOLATION OF NUCLEAR POWER PLANTS

ANDREW S. WHITTAKER^{†‡}, MANISH KUMAR[§], and MANISH KUMAR[§]

Department of Civil, Structural and Environmental Engineering, 212 Ketter Hall, University at Buffalo, State University of New York, Buffalo, NY 14260, U.S.A.

*Corresponding author. E-mail : awhittak@buffalo.edu

Received October 13, 2014

Seismic isolation is a viable strategy for protecting safety-related nuclear structures from the effects of moderate to severe earthquake shaking. Although seismic isolation has been deployed in nuclear structures in France and South Africa, it has not seen widespread use because of limited new build nuclear construction in the past 30 years and a lack of guidelines, codes and standards for the analysis, design and construction of isolation systems specific to nuclear structures.

The funding by the United States Nuclear Regulatory Commission of a research project to the Lawrence Berkeley National Laboratory and MCEER/University at Buffalo facilitated the writing of a soon-to-be-published NUREG on seismic isolation. Funding of MCEER by the National Science Foundation led to research products that provide the technical basis for a new section in ASCE Standard 4 on the seismic isolation of safety-related nuclear facilities. The performance expectations identified in the NUREG and ASCE 4 for seismic isolation systems, and superstructures and substructures are described in the paper. Robust numerical models capable of capturing isolator behaviors under extreme loadings, which have been verified and validated following ASME protocols, and implemented in the open source code OpenSees, are introduced.

KEYWORDS : Nuclear Power Plant; Seismic Isolation; Elastomeric Bearings; Sliding Bearings

1. INTRODUCTION

Seismic (base) isolation is a relatively mature technology for protecting structures from the effects of moderate and severe earthquake shaking, with key developments in the 1980s and 1990s. Although the technology has been widely deployed for buildings, bridges and certain classes of mission-critical infrastructure, it has yet to be routinely adopted for the seismic protection of safety-related nuclear structures, including nuclear power plants. The limited numbers of applications to nuclear structures to date have been in France and South Africa, for which synthetic rubber (neoprene) bearings, including flat sliders in some installations, have been used. The reasons for the limited use of seismic isolation include a) a significant downturn in nuclear power plant construction in the thirty-year period from 1980 to 2010, b) construction of nuclear

facilities in regions of low to moderate seismic hazard for which isolation is not necessarily needed, and c) the lack of consensus standards for the analysis and design of seismic isolation systems for nuclear facilities and companion requirements for testing of prototype and production bearings.

The nuclear energy renaissance, which began in the United States nearly a decade ago, and somewhat interrupted by the Fukushima nuclear accident and the recent availability and low price of natural gas, rekindled interest in the use of seismic isolation to protect nuclear structures from the effects of moderate to severe earthquake shaking. This renewed interest led the United States Nuclear Regulatory Commission (NRC) to fund a research project on the seismic isolation of nuclear power plant structures with an emphasis on large light water reactors. One component of the project is the preparation of a NUREG on seismic isolation, which should be published in the coming year. The NUREG will provide guidance on the analysis, design and construction of seismic isolation systems for nuclear power plants. The guidance is virtually identical to the mandatory provisions and commentary that will appear in Section 7.7 of the forthcoming edition of ASCE Standard 4 (ASCE, forthcoming), with the key difference being the definition of the beyond design basis earthquake.

[†]Correspondence to: Andrew S. Whittaker, Department of Civil, Structural and Environmental Engineering, 212 Ketter Hall, University at Buffalo, State University of New York, Buffalo, NY 14260, U.S.A.

*E-mail: awhittak@buffalo.edu

[‡]Professor, Chair and Director of MCEER

[§]PhD Candidates

Figure 1 identifies components of a seismically isolated nuclear structure as characterized in the forthcoming NUREG on seismic isolation (USNRC, forthcoming). The isolators (also termed isolator units and bearings) are assumed installed in a near horizontal plane beneath a basemat that supports the nuclear construction, which is defined as the *superstructure*. The isolators are installed atop pedestals and a foundation, which is defined as the *substructure*. The moat is a space in which the isolated superstructure can move without restriction in the event of earthquake shaking. Only horizontal isolation is considered because there are no viable three-dimensional isolation systems available in the marketplace at the time of this writing for large building structures such as nuclear power plants.

The NRC-funded research project is developing knowledge and tools to aid in the implementation of seismic isolation systems in nuclear power plants in the United States. Included in the topics for study are

- Preparation of a NUREG on seismic isolation
- Development of verified and validated models for elastomeric bearings
- Development of verified and validated models for sliding isolation systems
- Design procedures for displacement-restraint systems (or hard stops)
- Soil-structure-interaction analysis of seismically isolated nuclear power plants
- Aircraft impact analysis of seismically isolated nuclear structures

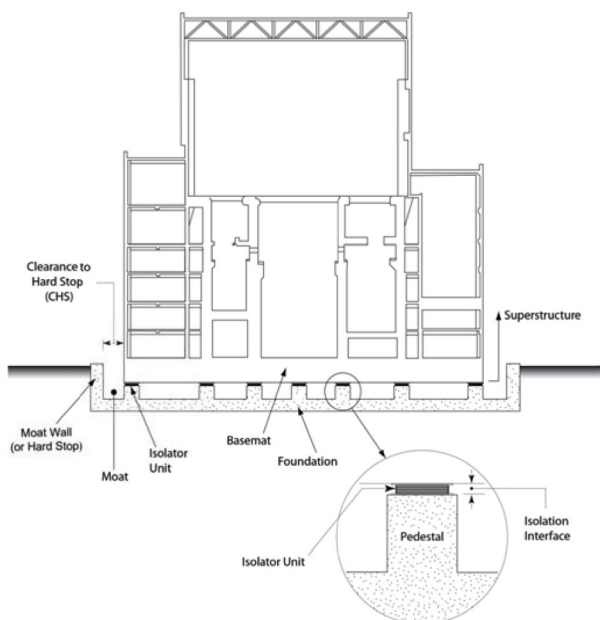


Fig. 1. Seismically Isolated Nuclear Power Plant (USNRC, forthcoming)

Some of the progress to date is documented in this paper. Kumar *et al.* (2013a, 2014a) and Kumar *et al.* (2013b, 2014b) and forthcoming MCEER reports document products of the project in greater detail than provided here. The following sections of this paper address aspects of the analysis and design of seismic isolation systems for safety-related nuclear structures in the United States. Section 2 introduces the performance expectations for seismic isolators and systems. The types of isolators identified for possible deployment in the United States are discussed in Section 3. Sections 4 and 5 introduce aspects of *verified* and *validated* models of elastomeric and sliding isolation systems.

2. PERFORMANCE OBJECTIVES

The performance expectations of Section 1.3 of ASCE 43 (ASCE, 2005) form the basis of the provisions of Section 7.7 of ASCE 4 (ASCE, forthcoming), namely, 1) 1% probability of unacceptable performance for 100% Design Basis Earthquake (DBE) shaking, and 2) 10% probability of unacceptable performance for shaking 150% of design basis. Beyond Design Basis Earthquake (BDBE) shaking is defined as 150% DBE shaking. Consistent with other sections of ASCE 4, seismic demands on the isolated superstructure are calculated at the 80th percentile for DBE shaking.

A significant difference between Section 7.7 of ASCE 4 and companion provisions for buildings (ASCE, 2010) and bridges (AASHTO, 2010) is the introduction of a physical stop. The stop, which can be a *moat* wall, is used to prevent excessive displacement of the isolation system and removes the isolation system from accident sequences involving earthquake shaking. The unrestricted travel (displacement) of the isolation system is defined as the clearance to the stop, CS. The stop need not be provided if the mean annual frequency of failure of the isolation system is so small that it can be screened out as part of a seismic probabilistic risk assessment, noting that screening frequencies will vary by country and regulator.

Table 1 summarizes the performance expectations for seismically isolated nuclear structures per the forthcoming edition of ASCE 4 (ASCE, forthcoming). The expectations presented in a similar table in the forthcoming NUREG are virtually identical expect for the definition of the beyond design basis earthquake. In the NUREG, beyond design basis shaking is defined as the greater of a) 167% of DBE shaking, and b) a Uniform Hazard Spectrum calculated for a return period of 100,000 years, all with a lower bound on the spectral acceleration at long periods. Hereafter the paper uses the ASCE 4 definition of BDBE shaking, which can be replaced by the more demanding NUREG definition for isolated nuclear power plants in the United States.

Hazard	Use	Isolation system			Other SSCs	Umbilical lines	Hard Stop or Moat
		Isolation system displacement	Performance	Acceptance criteria			
<p>DBE Response spectrum per Chapter 2</p>	<p>Production testing of isolators. Design loads for isolated superstructure. In-structure response spectra (ISRS).</p>	<p>Mean and 80th percentile isolation system displacements.</p>	<p>No damage to the isolation system for DBE shaking.</p>	<p>Production testing of each isolator for the 80th percentile isolation system and corresponding axial force. Isolators damaged by testing cannot be used for construction.</p>	<p>Conform to consensus materials standards for 80th percentile demands. Greater than 99% probability that component capacities will not be exceeded. Greater than 99% probability that the superstructure will not contact the moat.¹</p>	<p>Conform to ASME standards for 80th percentile demands; adjust ISRS per Section 6.2.3. Greater than 99% probability that component capacities will not be exceeded.</p>	<p>-</p>
<p>BDBE 150% of DBE</p>	<p>Prototype testing of isolators. Selecting moat width (or Clearance to Stop).</p>	<p>90th percentile isolation system displacement.²</p>	<p>Greater than 90% probability of the isolation system surviving BDBE shaking without loss of gravity-load capacity.</p>	<p>Prototype testing of a sufficient number of isolators for the CS displacement and the corresponding axial force. Isolator damage is acceptable but load-carrying capacity is maintained.</p>	<p>Greater than 90% probability that the superstructure will not contact the moat. Achieved by setting the moat width equal to or greater than the 90th percentile displacement. Greater than 90% probability that component capacities will not be exceeded.</p>	<p>Greater than 90% probability that component capacities will not be exceeded.</p>	<p>Clearance to Stop (CS) or moat width equal to or greater than the 90th percentile displacement. Damage to the moat is acceptable in the event of contact.</p>

1. Can be achieved by satisfying the requirement for BDBE shaking.
2. 90th percentile BDBE displacements may be calculated by multiplying the mean DBE displacement by a factor of 3.
3. The number of prototype isolators to be tested shall be sufficient to provide the required 90+-% confidence.

Table 1. Minimum ASCE 4 Performance Expectations for Seismically Isolated Nuclear Facilities

Analysis is performed for DBE and BDBE shaking of an isolated nuclear structure. Results of DBE analysis are used for a) calculating design loads on the superstructure, b) generating in-structure response spectra for design of structures, components and systems (SSCs), and c) establishing displacements for production testing of isolators. Results of BDBE analysis are used to a) select the required clearance to the physical stop, and b) establish displacements and forces for prototype testing of isolators.

Four performance statements for achieving the two performance objectives of ASCE 43 were assumed in the writing of Section 7.7 of ASCE Standard 4 (and the seismic isolation NUREG), namely, 1) individual isolators shall suffer no damage in DBE shaking, 2) the probability of the isolated nuclear structure impacting surrounding structure or the moat wall for 100% (150%) DBE shaking shall be 1% (10%) or less, 3) individual isolators shall sustain gravity and earthquake-induced axial loads at 90th percentile lateral displacements consistent with 150% DBE shaking, and 4) the probability of unacceptable performance in the isolated superstructure for 100% (150%) DBE shaking shall be 1% (10%) or less. Performance statement 1 is realized by production testing of each isolator supplied to a project for the 80th percentile DBE displacement and co-existing gravity and earthquake-induced axial forces. Analysis can be used in support of performance statement 2 provided that the isolators are modeled correctly and the ground motion representations are reasonable. Huang et al. (2009, 2012) showed that the 90th percentile displacement for 150% DBE shaking is greater than 99th percentile displacement for DBE shaking and so the former is used to establish the clearance to the stop, CS. Performance statement 3 is achieved by prototype testing of a limited number of isolators at a displacement equal to CS and co-existing axial forces, noting that an isolation system is composed of tens to hundreds of isolators and that failure of an isolation system would have to involve the simultaneous failure of a significant percentage of the isolators in the system. Performance statement 4 is checked by analysis of the capacity of the isolated superstructure at 100% DBE and BDBE shaking

using procedures presented in Section 1 of ASCE 4 and in the commentary to ASCE 43. If the probabilities of failure at DBE and BDBE shaking exceed the limits of Section 1.3 of ASCE 43, the capacity (strength) of the isolated superstructure is increased until the performance statement is achieved. Adequate performance of the foundation is achieved by designing for forces delivered by the isolation system at displacement CS.

3. ISOLATORS AND ISOLATION SYSTEMS FOR US APPLICATIONS

Three types of isolators have been qualified for use in safety-related nuclear structures in the United States: low damping (natural) rubber (LDR) isolators, lead (natural) rubber (LR) isolators, and the Friction Pendulum (FP) sliding isolator. Each has been tested extensively in the United States, can be modeled for nonlinear response-history analysis, and has been deployed in mission-critical structures in the United States. The mechanical characteristics of these isolators (linear and bilinear) underpin the rules set forth in Section 7.7 of ASCE 4 (and the seismic isolation NUREG). The assumed hysteretic response of LR and FP bearings in a horizontal direction is presented in Figure 2.

Low-damping (LD) elastomeric bearings are composed of alternating layers of natural rubber and steel, and can be modeled as viscoelastic components. The shear modulus of the rubber ranges between 60 psi and 120 psi. The equivalent viscous damping is between 2 and 4% of critical. Lead-rubber (LR) elastomeric bearings are constructed similarly to low-damping rubber bearings but include a central lead core to dissipate earthquake-induced energy. The hysteresis loop for the LR bearing is bilinear per Figure 2 and defined by a zero-displacement force intercept, Q_d , an elastic stiffness, K_u , and a second-slope stiffness, K_d , where W is the supported weight. Sliding bearings with restoring force provided by gravity also have the hysteresis loop of Figure 2. In the Friction Pendulum™ (FP) family of bearings, the second-slope stiffness is related to the supported weight and the radius

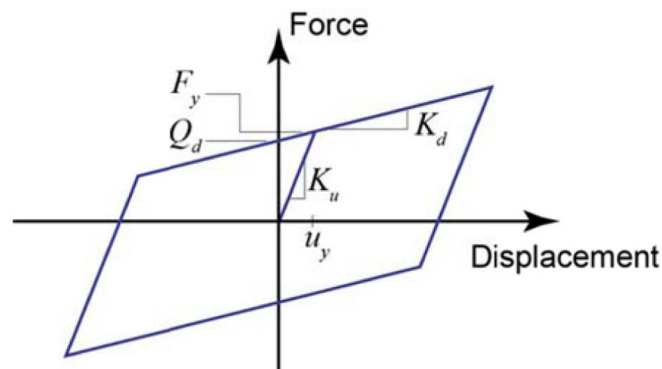


Fig. 2. Assumed Hysteretic Response of LR and FP Bearings in a Horizontal Direction

of curvature of the sliding surfaces. Constantinou et al. (2007) and Naeim and Kelly (1999) provide information on LD, LR and FP seismic isolators. Huang et al. (2008, 2009, 2010, 2012) provide data and information in support of the isolation of nuclear structures and the provisions of Section 7.7 of ASCE 4. Constantinou et al. (1999, 2007), Thompson *et al.* (2000) and Morgan *et al.* (2001) provide the data used by Huang *et al.* (2009, 2012) to characterize the impact of variations in isolator material properties on the displacement response of seismic isolation systems.

Other types of isolators from the three mentioned above are not precluded from use in safety-related nuclear structures in the United States. Rather, the following tasks must be undertaken to qualify another type of isolator (or isolation system) for use in a safety-related nuclear structure in the United States:

1. Dynamic testing of full-scale (prototype) isolators for compressive and tensile axial loads and bidirectional horizontal motion at amplitudes of displacement expected for beyond design basis ground motions in regions of moderate and high seismic hazard;
2. Development of *verified* and *validated* numerical models capable of predicting the results of dynamic testing of prototype isolators, including deterioration of hysteresis due to energy dissipation during earthquakes;
3. Demonstration through basic chemistry, laboratory tests and field applications that the mechanical properties of the isolators do not change by more than 20% over a 50- to 100-year period in the temperature range of 40°F to 80°F;
4. System-level testing of the isolation system using three translational components of earthquake ground motion;
5. Verification and validation of numerical tools and codes to predict the seismic response of the isolation system; and
6. Deployment of an isolation system composed of the isolators in mission-critical structures.

Section 7.7 requires tasks 1 through 5 to be performed by experienced persons, independent of the isolator manufacturer. Hybrid isolation systems involving different types of bearing (e.g., sliding and elastomeric) are not permitted.

4. NUMERICAL MODELING OF ELASTOMERIC BEARINGS

4.1 Introduction

Traditional nuclear power plant design involving reinforced concrete has involved strength design for design basis (or safe shutdown) earthquake shaking and the use of ductile details to provide inelastic deformation capacity in the event of shaking more intense than design basis.

Seismic analysis is performed for design basis shaking. Inelastic action was presumed to develop in those components detailed for ductile response. Rudimentary evaluation in the form of static nonlinear (pushover) analysis is performed in selected cases to support safety cases.

The seismic isolation of a safety-related nuclear structure should force inelastic response into the bearings beneath the superstructure. This concentration of inelastic response into a singleton (the isolation system) led the writers of nuclear standards and regulators in the United States to require explicit analysis for beyond design basis shaking, where such shaking is associated with return periods of between 10,000 and 100,000 years for which seismic spectral demand will be significant, even for regions of low seismic hazard. The need for confirmation of acceptable performance in beyond design basis shaking was reinforced by the Fukushima nuclear accident.

The intense shaking that may be associated with beyond design basis shaking in regions of moderate to high seismic hazard, and the concentration of inelastic action in the bearings of a seismically isolated nuclear structure, led the NRC to support the development of numerical models for seismic isolators under extreme loadings. These models, for elastomeric and sliding isolation systems of the types described in Section 3, were developed as part of the research project introduced previously, which was undertaken by MCEER and the University at Buffalo through a grant administered by Lawrence Berkeley National Laboratory. The following subsections describe the model that was *verified* and *validated* for elastomeric isolators. Section 5 presents companion information on sliding isolators.

The models of elastomeric bearings used for analysis of safety-related nuclear structures under design and beyond design basis earthquake shaking may include considerations of

1. Coupled bidirectional motion in horizontal directions
2. Coupling of vertical and horizontal motion
3. Cavitation and post-cavitation behavior in tension
4. Strength degradation under cyclic tensile loading due to cavitation
5. Variation in critical buckling load capacity due to lateral displacement
6. Strength degradation in cyclic shear loading due to heating of the lead core

A numerical model capable of accommodating these six behaviors did not exist and was developed as part of the NRC-funded research project, substantially expanding existing capabilities to address extreme earthquake loadings. The model was verified and validated following ASME best practices (ASME, 2006), and implemented in OpenSees (McKenna et al., 2006) to enable use by researchers and the design professional community. Complete details are provided in Kumar et al. (2013a, 2014a) and pertinent information is presented below.

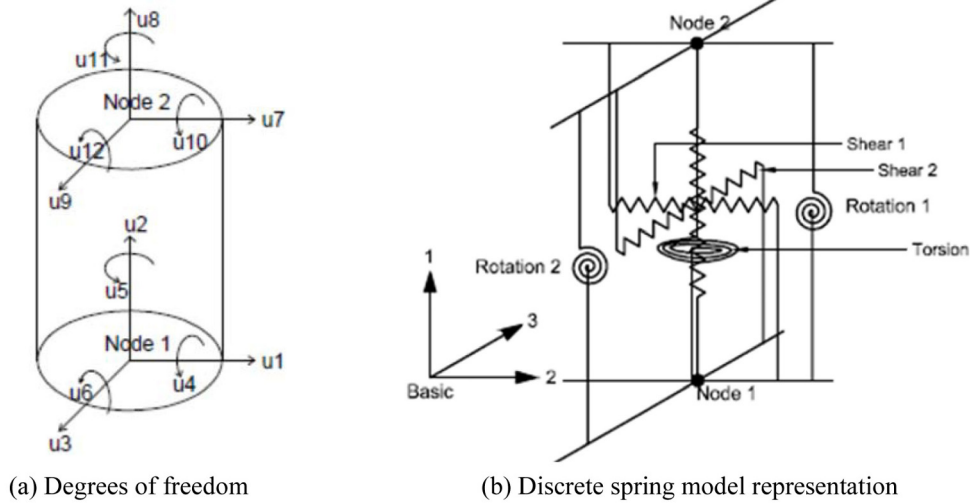


Fig. 3. Physical Model of an Elastomeric Bearing (Kumar *et al.*, 2014a)

4.2 Physical Model of Elastomeric Bearings

The physical model of an elastomeric bearing is considered as a two-node, twelve degrees-of-freedom discrete element. The two nodes are connected by six springs that represent the mechanical behavior in the six basic directions of a bearing. The degrees of freedom and discrete spring representation of an elastomeric bearing is shown in Figure 3.

The general form of element force vector, f_b , and element stiffness matrix, K_b , for the element representation presented above is given by Eqn. (1).

$$f_b = \begin{bmatrix} Axial \\ Shear1 \\ Shear2 \\ Torsion \\ Rotation1 \\ Rotation2 \end{bmatrix}; \quad (1)$$

$$K_b = \begin{bmatrix} Axial & 0 & 0 & 0 & 0 & 0 \\ 0 & Shear1 & Shear12 & 0 & 0 & 0 \\ 0 & Shear21 & Shear2 & 0 & 0 & 0 \\ 0 & 0 & 0 & Torsion & 0 & 0 \\ 0 & 0 & 0 & 0 & Rotation1 & 0 \\ 0 & 0 & 0 & 0 & 0 & Rotation2 \end{bmatrix}$$

The coupling of the two shear springs is considered directly by using a coupled bidirectional model. All other springs are uncoupled. The couplings of the vertical and horizontal directions are considered indirectly by using expressions for mechanical properties in one direction that are dependent on the response parameters in the other direction. Linear uncoupled springs are adopted for the torsion and the two rotational springs as they are not

expected to significantly affect the response of an elastomeric bearing. The off-diagonal terms due to coupling between axial and shear, and axial and rotation, are ignored. The expression for mechanical properties, including stiffness and buckling load capacity, are derived using explicit considerations of geometric nonlinearity due to large displacement effects.

The physical model and the mechanical properties of elastomeric bearings in horizontal and vertical direction are discussed here for low damping rubber (LDR) bearing, lead rubber (LR) bearing, and high damping rubber (HDR).

4.3 Behavior under Axial Loading

4.3.1 Tension

The phenomenological model is presented in Kumar *et al.* (2014a) is used here to describe the behavior of elastomeric isolation bearings in tension, including the cavitation and post-cavitation behavior. The cavitation force in an elastomeric bearing is calculated as $F_c = 3GA_o$, where A_o is the bonded rubber area before cavitation in the rubber. The shear modulus, G , is obtained experimentally from testing at a moderate shear strains under nominal axial loads. The post-cavitation force, F , at tensile deformation, u , is given by:

$$F = F_c \left[1 + \frac{1}{kT_r} (1 - e^{-k(u-u_c)}) \right] \quad (2)$$

where k is the cavitation parameter, which describes the post-cavitation variation of tensile stiffness, and T_r is the total rubber thickness.

Cavitation in an elastomeric bearing is accompanied by irreversible damage due to the formation of micro cracks in the volume of rubber. When a bearing is loaded beyond the point of cavitation and unloaded, it returns along a new path and the cavitation strength is

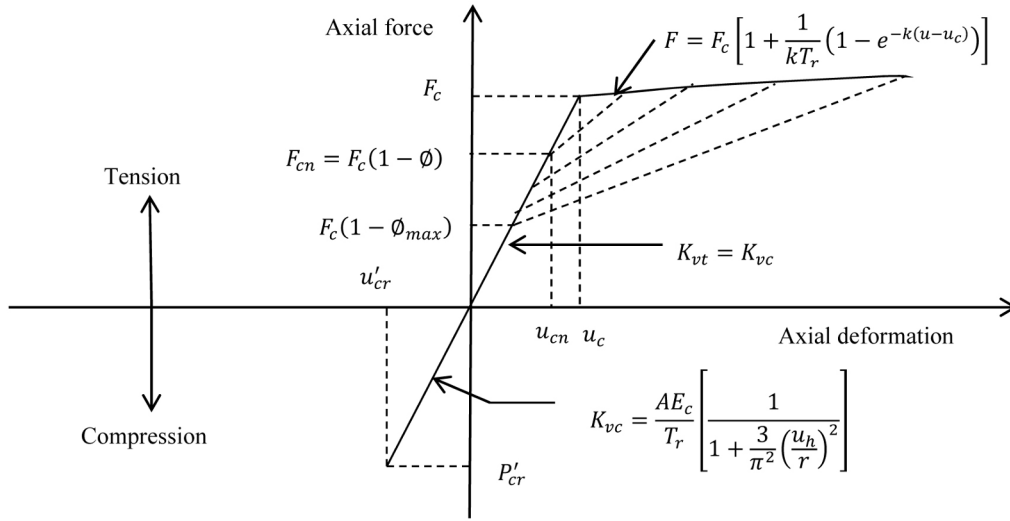


Fig. 4. Mathematical Model of an Elastomeric Bearing in the Axial Direction (Kumar *et al.*, 2014a)

reduced. Subsequent loading follows the latest unloading path elastically until strain exceeds the past maximum value u_{\max} , below which loading has the effect of only opening and closing of existing cavities within the rubber. Once loading exceeds the past maximum value of tensile strain, the formation of new cavities leads to increased damage, and follows the post cavitation behavior defined previously by Eqn. (2). Upon load reversal, it again traces back a new unloading path and the cavitation strength is further reduced. Unloading paths can be approximated by straight lines between the points of maximum strain (F_{\max} , u_{\max}) and reduced cavitation strength (F_{cn} , u_{cn}). Points (F_{\max} , u_{\max}) and (F_{cn} , u_{cn}) change with an increasing number of cycles. To capture this behavior mathematically, a damage index ϕ is defined such that the updated cavitation strength as a function of initial cavitation strength is given by the expression, $F_{cn} = F_c(1-\phi)$. The damage index ϕ calculated using:

$$\phi = \phi_{\max} \left(1 - e^{-a \left(\frac{u-u_c}{u_c} \right)} \right) \quad (3)$$

where a is a strength degradation parameter that defines the rate of damage and ϕ_{\max} is the maximum damage that can be expected in a bearing.

4.3.2 Compression

The two-spring model (Koh and Kelly, 1987), validated experimentally by Warn *et al.* (2007), is used here to model the behavior of elastomeric bearing in axial compression. The coupling of horizontal and vertical behavior is considered by: 1) dependence of axial stiffness on lateral displacement, and 2) variation of shear stiffness with axial load. The vertical, K_v , and horizontal, K_H , stiffness of the elasto-

meric bearing obtained from the two-spring model are:

$$K_v = \frac{AE_c}{T_r} \left[1 + \frac{3}{\pi^2} \left(\frac{u_h}{r} \right)^2 \right]^{-1}; \quad (4)$$

$$K_H = \frac{GA}{T_r} \left[1 - \left(\frac{P}{P_{cr}} \right)^2 \right] = K_{H0} \left[1 - \left(\frac{P}{P_{cr}} \right)^2 \right]$$

where E_c is the compression modulus of the bearing, u_h is the lateral displacement of the bearing, r is the radius of gyration of the bonded rubber area, K_{H0} is the horizontal stiffness at zero axial load, P is the instantaneous value of axial load, and P_{cr} is the instantaneous value of critical buckling load. The calculation of E_c for different bearing shapes is discussed in Constantinou *et al.* (2007).

The load, P_{cr} , decreases with increasing lateral displacement. The area-reduction method considers the dependence of P_{cr} on lateral displacement and provides conservative results (Buckle and Liu, 1993). The model suggested by Warn *et al.* (2006, 2007) is considered here, which uses a bilinear approximation of the area-reduction method and takes into account the finite buckling capacity of a bearing at zero overlap area. The reduced critical load is given by:

$$P'_{cr} = \begin{cases} P_{cr} \frac{A_r}{A} & \text{for } \frac{A_r}{A} \geq 0.2 \\ 0.2P_{cr} \frac{A_r}{A} & \text{for } \frac{A_r}{A} < 0.2 \end{cases} \quad (5)$$

A mathematical model of an elastomeric bearing in the axial direction is presented in Figure 4. The model uses three unknown parameters: 1) a cavitation parameter, k , 2) a strength degradation parameter, a , and 3) a damage index, ϕ_{\max} .

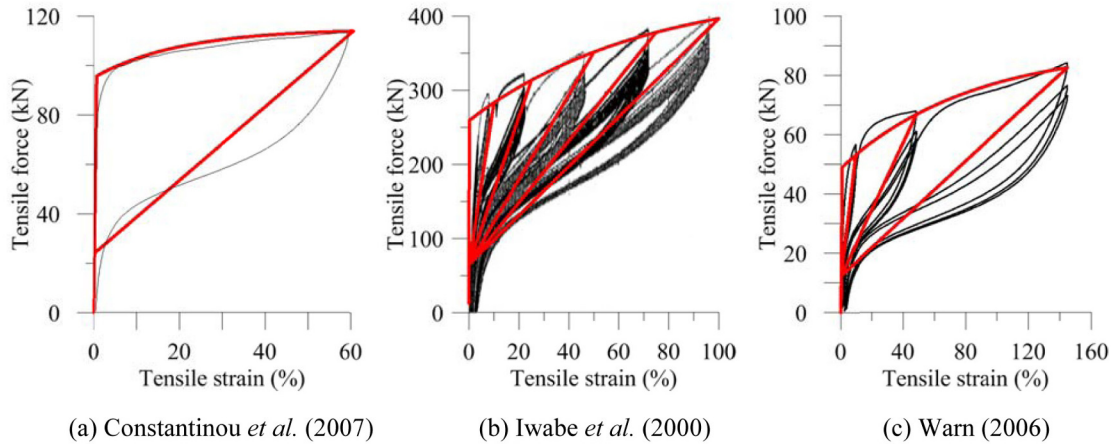


Fig. 5. Comparison of Experimental and Numerical Results for LDR Bearings in Tension (Kumar *et al.*, 2014a)

Table 1. Properties of the Bearings used for Experimental Comparison

	Constantinou <i>et al.</i> (2007)	Iwabe <i>et al.</i> (2000)	Warn <i>et al.</i> (2006)
Diameter, mm	250	500	164
Shape factor, S	9.8	33	10.2
Cavitation parameter, k	60	15	20
Max. damage index, ϕ_{\max}	0.75	0.75	0.75
Degradation parameter, a	1.0	1.0	1.0

4.4 Behavior under Shear Loading

The behavior of elastomeric bearings in shear is well established, and two bidirectional hysteretic models are used to model the behavior of elastomeric bearings in shear. The Bouc-Wen model (Park *et al.*, 1986; Wen, 1976) extended for analysis of seismic isolations under bidirectional motion by Nagarajaiah *et al.* (1991) is used for LDR and LR bearings. The model proposed by Grant *et al.* (2004) is used to model the behavior of HDR bearings. The strength degradation in a LR bearing due to heating of lead core is incorporated using model proposed by Kalpakidis *et al.* (2010). The effective shear modulus of elastomeric bearings is obtained from experimental data.

4.5 Implementation and Experimental Validation

The mathematical models of LDR, LR, and HDR bearings are implemented in OpenSees as three user elements, ElastomericX, LeadRubberX and HDR, respectively.

The tensile behavior of elastomeric bearings is validated using three sets of experimental data, as shown in Figure 5. The cavitation parameter, k , and the damage index, ϕ_{\max} , were obtained by visual calibration of the mathematical model with experimental data. The strength degradation parameter, a , was assumed to be

unity. The details of the bearings and the values of parameters estimated by calibration against experimental data are presented in Table 1.

The behavior of elastomeric bearings under shear and compression is also well understood, as described previously. Models to capture the degradation in strength of LR bearings due to heating of the lead core under cyclic shear loading have been developed and validated by Kalpakidis *et al.* (2010). Herein, these models were coded in OpenSees and verified against analytical solutions and validated against the experimental data used by Kalpakidis.

5. NUMERICAL MODELING OF SLIDING BEARINGS

5.1 Introduction

Friction Pendulum™ (FP) bearings have been widely used to seismically isolate structures in the United States and abroad. This family of hemispherical sliding bearings includes single, double and triple concave variants. The single concave FP bearing, which is studied here, comprises a sliding surface of polished stainless steel and an articulated slider coated with a PTFE-type composite

material. Figure 6 presents a section through a FP bearing.

Models of the FP sliding bearing used for analysis of safety-related nuclear structures under design and beyond design basis earthquake shaking may include considerations of

1. Coupled bidirectional motion in horizontal directions
2. Coupling of vertical and horizontal motion
3. Strength degradation in cyclic shear loading due to heating of the sliding surface

As proposed here, the single concave FP bearing cannot resist net tensile loadings although variants have been tested to do so (Marin *et al.* 2009). A numerical model capable of accommodating these three behaviors was developed as part of the NRC-funded project, substantially expanding the existing models of FP-type bearings. The model was verified and validated, unlike prior models, following ASME best practices (ASME, 2006) and is being implemented in OpenSees. Complete details are provided in Kumar *et al.* (2013b, 2014b).

5.2 Force-displacement Behavior

The bilinear curve of Figure 2 describes the force-displacement behavior of an FP bearing with constant values of coefficient of sliding friction and axial load, subjected to a monotonic lateral displacement. The behavior is characterized by a characteristic strength, Q_d , and a post-yield stiffness K_d . The characteristic strength is the product of the coefficient of friction and the axial load, and the post-yield stiffness is the ratio of the axial load on the bearing to the radius of curvature.

In reality, during earthquake shaking, the axial load changes continuously due to the vertical component of ground motion and the superstructure's response, and the coefficient of friction changes continuously with sliding velocity, axial pressure and temperature at the sliding surface. The temperature at a location on the sliding surface at a given instant is a function of histories of axial load, sliding velocity and coefficient of friction, and the path previously traversed by the slider on the sliding surface. A robust model of a sliding bearing should capture these dependencies. The following section discusses the relationships between coefficient of friction and sliding velocity, temperature, and axial pressure.

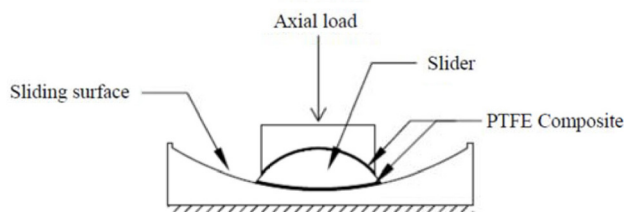


Fig. 6. Section Through a Single Concave Friction Pendulum™ (FP) Bearing (Kumar *et al.*, 2014b)

5.3 Characterizing the Evolution of the Coefficient of Friction

The coefficient of friction changes with sliding velocity due to the viscous nature of the PTFE-type composite coating. The coefficient increases with an increase in velocity at small velocities and approaches a constant value at higher velocities (e.g., Mokha *et al.*, 1988). The high-velocity coefficient of friction decreases with increase in axial pressure, whereas the small-velocity coefficient of friction remains almost unaffected (e.g., Constantinou *et al.*, 1993). Expressions to describe the variations in coefficient of friction with sliding velocity and axial pressure have been proposed (e.g., Tsopelas *et al.*, 1994; Dao *et al.*, 2013) and incorporated in software such as SAP2000 (CSI, 2013) and OpenSees (McKenna *et al.*, 2006).

The coefficient of friction decreases with increase in the temperature on the sliding surface due to frictional heating, which is attributed to softening in the PTFE-type composite material. There is limited experimental data on variation in the coefficient of sliding friction with temperature on the sliding surface (e.g., Constantinou *et al.*, 2007). The pressure-, temperature- and velocity-dependences of the coefficient of friction are accounted for by factors for pressure k_p , temperature, k_T , and velocity, k_v , as follows (Kumar *et al.*, 2014b):

$$k_v = 1 - 0.5e^{-av} \quad (6)$$

$$k_T = 0.79 \times \left(0.70^{T/50} + 0.40 \right) \quad (7)$$

$$k_p = 0.70^{(p-p_o)/50} \quad (8)$$

where a determines the rate at which coefficient of friction increases with increase in sliding velocity v , T is temperature at the sliding surface, p is the instantaneous axial pressure on the bearing, and p_o is the reference static axial pressure at which the coefficient of friction is measured at a high velocity of sliding. The factors k_v and k_p are obtained assuming the small-velocity coefficient of friction is one-half the high-velocity coefficient of friction at all levels of axial pressure. The factor k_T is based on the assumption that the ratios of the coefficients of friction at temperatures of -40°C, 20°C and 250°C is 3:2:1. The three factors are discussed in detail in Kumar *et al.* (2014b).

A reference coefficient of friction, μ_{ref} , is defined as the coefficient of friction at the axial pressure p_o , measured at a high-velocity of sliding with the temperature at the sliding surface of T_o (20°C for this study). The coefficient of friction adjusted for the three effects, $\mu(p, T, v)$, is then computed as the product of μ_{ref} and the three factors:

$$\mu(p, T, v) = \mu_{ref} k_p k_T k_v \quad (9)$$

The temperature, T , at an instant at a location on the sliding surface is computed by convolving the heat flux history with a decay function ($1/\sqrt{t}$). Three assumptions

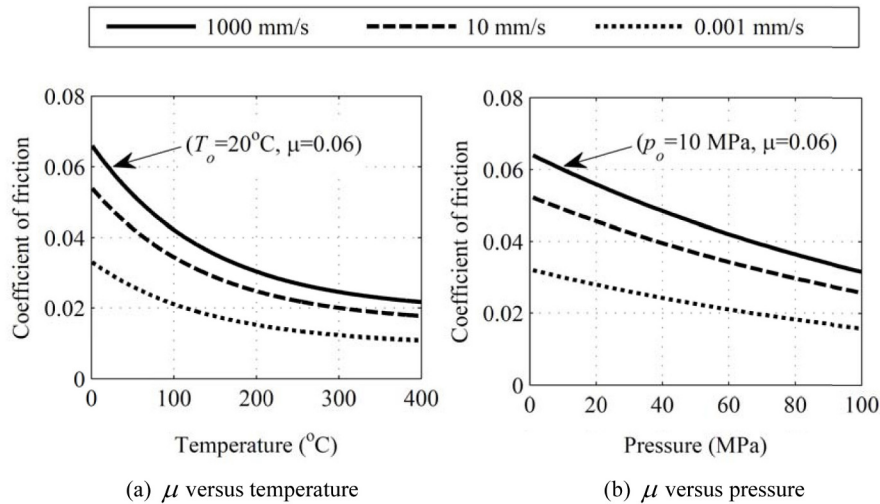


Fig. 7. Variation in the Coefficient of Friction with Sliding Velocity, Axial Pressure and Temperature at the Sliding Surface (Kumar *et al.*, 2014b)

are made: 1) the heat generated at the sliding surface is transferred to the sliding surface only, 2) conditions of an infinite half-space for heat conduction are realized, and 3) temperature at the center of the sliding surface represents the temperature at the sliding surface. These assumptions are discussed in detail in Constantinou *et al.* (2007) and Kumar *et al.* (2014b). The heat flux at a location is the product of coefficient of friction, sliding velocity and axial pressure when the slider is over the location and zero otherwise.

Figure 7a plots the coefficient of friction against temperature and Figure 7b plots the coefficient of friction against axial pressure for three values of sliding velocity (=1000 mm/s, 10 mm/s and 0.001 mm/s). If the temperature at the sliding surface rises from 20°C to a maximum of 250°C, the high-velocity coefficient of friction will vary between 0.06 and 0.03, for a constant axial pressure. Similarly, if the axial pressure on the bearing ranges between 2 MPa and 18 MPa, the high-velocity coefficient of friction will vary between 0.064 and 0.057.

5.4 Intra-earthquake Evolution of the Coefficient of Friction

Single FP bearings with a sliding period of 3 s, μ_{ref} of 0.06, and p_o of 10 MPa and 50 MPa were subjected to a set of thirty ground motions representing seismic hazard with a return period of 10,000 years for the site of the Diablo Canyon nuclear generating station. Information on these ground motions is provided in Huang *et al.* (2009). Figure 8a plots the force-displacement response in a horizontal direction for the bearing with p_o of 10 MPa and friction at the sliding surface described by Coulomb model ($k_p=1$; $k_T=1$; $k_v=1$) subjected to one of the 30 ground motions. Figure 8c presents the response for the case where the friction model accounts for the

effects of heating only. The peak displacements in the two panels are 290 mm and 310 mm, respectively. The heating effects are much more significant at $p_o = 50$ MPa. The peak displacements corresponding to the two friction models are 290 mm (Figure 8b) and 510 mm (Figure 8d), respectively. The velocity and pressure dependencies of the coefficient of friction do not significantly affect the peak displacements or the transmitted forces, as described in Kumar *et al.* (2014b).

6. CLOSING REMARKS

Seismic isolation is a viable strategy for protecting safety-related nuclear structures from the effects of moderate to severe earthquake shaking but it has not been widely adopted because of limited nuclear construction in the past 30 years and a lack of guidelines, codes and standards for the analysis, design and construction of isolation systems specific to nuclear structures.

Research funding from the United States Nuclear Regulatory Commission to the Lawrence Berkeley National Laboratory and MCEER/University at Buffalo has facilitated the writing of a soon-to-be-published NUREG on seismic isolation. Funding of MCEER by the National Science Foundation led to research products that provide the technical basis for a new section in ASCE Standard 4 on the seismic isolation of safety-related nuclear facilities. The performance expectations identified in the NUREG and ASCE 4 for seismic isolation systems, and superstructures and substructures, are identified and their technical bases are provided. Key to the implementation of the technology is the development of verified and validated numerical models of isolators capable of capturing behaviors under extreme loadings. Such models are in-

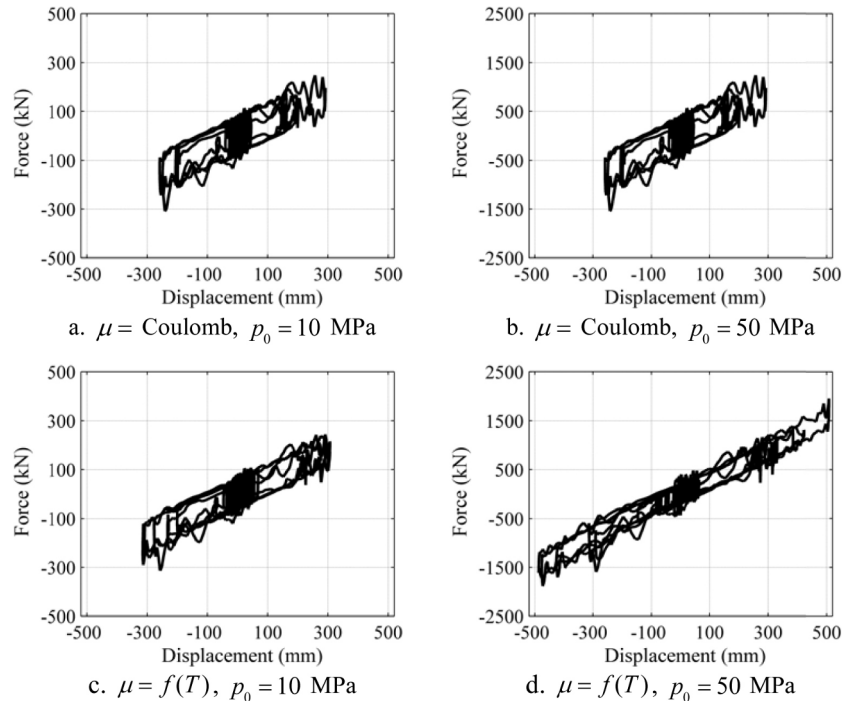


Fig. 8. Force-displacement Histories of an FP Bearing in the Y Direction with Sliding Isolation Period of 3 s and Reference Coefficient of Friction 0.06, Subjected to an Earthquake Ground Motion

roduced in the paper and have been implemented into the open source code OpenSees as new user elements.

ACKNOWLEDGEMENTS

This research project is supported by a grant to MCEER from the United States Nuclear Regulatory Commission and the Lawrence Berkeley National Laboratory (LBNL). This financial support is gratefully acknowledged. The authors thank Dr. Robert Budnitz of LBNL for his guidance on the project, Professor Michael Constantinou of the University at Buffalo for his advice on modeling elastomeric and sliding isolators, and former graduate students Dr. Ioannis Kalpakidis of Energo Engineering and Dr. Gordon Warn of Penn State University for providing test data on elastomeric bearings.

REFERENCES

- [1] American Association of State Highway and Transportation Officials (AASHTO). (2010). "Guide specifications for seismic isolation design." Washington, D.C.
- [2] American Concrete Institute (ACI). (2006). "ACI 349-06: Code requirements for nuclear safety-related structures." Farmington Hills, MI.
- [3] American Society of Civil Engineers (ASCE). (2005). "Seismic design criteria for structures, systems, and components in nuclear facilities." *ASCE/SEI 43-05*, Reston, VA.
- [4] American Society of Civil Engineers (ASCE). (2010). "Minimum design loads for buildings and other structures." *ASCE 7-10*, Reston, VA
- [5] American Society of Civil Engineers (ASCE). (forthcoming). "Seismic analysis of safety-related nuclear structures." *ASCE/SEI 4-***, Reston, VA.
- [6] American Society of Mechanical Engineers (ASME). (2006). "Guide for verification and validation in computational solid mechanics." *ASME V&V 10-2006*, New York, NY.
- [7] Buckle, I. G., and Liu, H. (1993). "Stability of elastomeric seismic isolation systems." *Proceedings: Seminar on Seismic Isolation, Passive Energy Dissipation, and Control*, Redwood City, California, 293-305.
- [8] Computers and Structures Incorporated (CSI). (2013). "Computer program SAP2000, Version 15.2.1." Berkeley, California.
- [9] Constantinou, M. C., Tsopeles, P., Kim, Y.-S., and Okamoto, S. (1993). "NCEER-Taisei Corporation research program on sliding seismic isolation systems for bridges: Experimental and analytical study of a Friction Pendulum System (FPS)." NCEER-93-0020, National Center for Earthquake Engineering Research, Buffalo, NY.
- [10] Constantinou, M. C., Tsopeles, P., Kasalanati, A., and Wolff, E. D. (1999). "Property modification factors for seismic isolation bearings." MCEER-99-0012, Multidisciplinary Center for Earthquake Engineering Research, Buffalo, NY.
- [11] Constantinou, M. C., Whittaker, A. S., Kalpakidis, Y., Fenz, D. M., and Warn, G. P. (2007). "Performance of seismic isolation hardware under service and seismic loading." MCEER-07-0012, Multidisciplinary Center for Earthquake Engineering Research, Buffalo, NY.
- [12] Dao, N. D., Ryan, K. L., Sato, E., and Sasaki, T. (2013). "Predicting the displacement of Triple Pendulum™ bearings in a full-scale shaking experiment using a three-dimensional element." *Earthquake Engineering & Structural Dynamics*, 42(11), 1677-1695.

- [13] Grant, D. N., Fenves, G. L., and Whittaker, A. S. (2004). "Bidirectional modeling of high-damping rubber bearings." *Journal of Earthquake Engineering*, 8, 161-185.
- [14] Huang, Y.-N., Whittaker, A. S., and Luco, N. (2008). "Performance assessment of conventional and base-isolated nuclear power plants for earthquake and blast loadings." MCEER-08-0019, Multidisciplinary Center For Earthquake Engineering Research, Buffalo, NY.
- [15] Huang, Y.-N., Whittaker, A. S., Kennedy, R. P., and Mayes, R. L. (2009). "Assessment of base-isolated nuclear structures for design and beyond-design basis earthquake shaking." MCEER-09-0008, Multidisciplinary Center For Earthquake Engineering Research, Buffalo, NY.
- [16] Huang, Y.-N., Whittaker, A. S., and Luco, N. (2010). "Seismic performance assessment of base-isolated safety-related nuclear structures." *Earthquake Engineering and Structural Dynamics*, 39(13), 1421-1442.
- [17] Huang, Y.-N., Whittaker, A. S., Kennedy, R. P., and Mayes, R. L. (2012). "Response of base-isolated nuclear structures for design and beyond-design basis earthquake shaking." *Earthquake Engineering & Structural Dynamics*, 42(3), 339-356.
- [18] Iwabe, N., Takayama, M., Kani, N., and Wada, A. (2000). "Experimental study on the effect of tension for rubber bearings." *Proceedings: 12th World Conference on Earthquake Engineering*, New Zealand.
- [19] Kalpakidis, I. V., Constantinou, M. C., and Whittaker, A. S. (2010). "Modeling strength degradation in lead-rubber bearings under earthquake shaking." *Earthquake Engineering and Structural Dynamics*, 39(13), 1533-1549.
- [20] Koh, C. G., and Kelly, J. M. (1987). "Effects of axial load on elastomeric isolation bearings." EERC/UCB 86/12, Earthquake Engineering Research Center, University of California, Berkeley, CA.
- [21] Kumar, M., Whittaker, A., and Constantinou, M. (2013a). "Mechanical properties of elastomeric seismic isolation bearings for analysis under extreme loadings." *Transactions, 22nd International Conference on Structural Mechanics in Reactor Technology (SMiRT 22)*, San Francisco, California.
- [22] Kumar, M., Whittaker, A. S., and Constantinou, M. C. (2013b). "Response prediction for friction pendulum bearings considering the dependence of friction on axial pressure, temperature and velocity." *Transactions, 22nd International Conference on Structural Mechanics in Reactor Technology (SMiRT 22)*, San Francisco, CA.
- [23] Kumar, M., Whittaker, A., and Constantinou, M. C. (2014a). "An advanced numerical model of elastomeric seismic isolation bearings." *Earthquake Engineering & Structural Dynamics*, Published online, DOI: 10.1002/eqe.2431.
- [24] Kumar, M., Whittaker, A., and Constantinou, M. C. (2014b). "Friction in sliding isolation bearings." *Earthquake Engineering & Structural Dynamics*, Paper submitted for review and possible publication.
- [25] Marin, C. C., Whittaker, A. S., and Constantinou, M. C. (2009). "Experimental study of the XY-Friction Pendulum bearing for bridge applications." *Journal of Bridge Engineering*, Vol. 14, No. 3, pp. 193-202.
- [26] McKenna, F., Fenves, G., and Scott, M. (2006). "Computer Program OpenSees: Open system for earthquake engineering simulation." Pacific Earthquake Engineering Center, University of California, Berkeley, CA., (<http://opensees.berkeley.edu>).
- [27] Mokha, A., Constantinou, M. C., and Reinhorn, A. M. (1988). "Teflon bearings in aseismic base isolation: experimental studies and mathematical modeling." NCEER-88-0038, National Center for Earthquake Engineering Research, Buffalo, NY.
- [28] Morgan, T., Whittaker, A. S., and Thompson, A. C. (2001). "Cyclic behavior of high-damping rubber bearings." *Proceedings: Fifth World Congress on Joints, Bearings and Seismic Systems for Concrete Structures*, American Concrete Institute, Rome, Italy.
- [29] Naeim, F., and Kelly, J. M. (1999). "Design of seismic isolated structures: from theory to practice." John Wiley & Sons, NY.
- [30] Nagarajaiah, S., Reinhorn, A. M., and Constantinou, M. C. (1991). "Nonlinear dynamic analysis of 3D-base-isolated structures." *Journal of Structural Engineering*, 117(7), 2035-2054.
- [31] Park, Y. J., Wen, Y. K., and Ang, A. H. S. (1986). "Random vibration of hysteretic systems under bi-directional ground motions." *Earthquake Engineering & Structural Dynamics*, 14(4), 543-557.
- [32] Thompson, A. C. T., Whittaker, A. S., Fenves, G. L., and Mahin, S. A. (2000). "Property modification factors for elastomeric seismic isolation bearings." *Proceedings: 12th World Conference on Earthquake Engineering*, Auckland, New Zealand.
- [33] Tsopelas, P. C., Constantinou, M. C., and Reinhorn, A. M. (1994). "3D-BASIS-ME: Computer program for nonlinear dynamic analysis of seismically isolated single and multiple structures and liquid storage tanks." NCEER-94-0010, National Center for Earthquake Engineering Research, Buffalo, NY.
- [34] United States Nuclear Regulatory Commission (USNRC). (forthcoming). "Technical considerations for seismic isolation of nuclear facilities." *NUREG-**, Washington DC.
- [35] Warn, G. P., and Whittaker, A. S. (2006). "A study of the coupled horizontal-vertical behavior of elastomeric and lead-rubber seismic isolation bearings." MCEER-06-0011, Multidisciplinary Center for Earthquake Engineering Research, Buffalo, NY.
- [36] Warn, G. P., Whittaker, A. S., and Constantinou, M. C. (2007). "Vertical stiffness of elastomeric and lead-rubber seismic isolation bearings." *Journal of Structural Engineering*, 133(9), 1227-1236.
- [37] Wen, Y.-K. (1976). "Method for random vibration of hysteretic systems." *Journal of the Engineering Mechanics Division*, 102(2), 249-263.